AD-A152 396 APPENDAGE EFFECTS ON PROPELLER INFLOW(U) SCIENCE APPLICATIONS INTERNATIONAL CORP ANNAPOLIS MD G H CHRISTOPH ET AL. 15 JAN 85 SAIC-85/1008 1/1

UNCLASSIFIED N00014-84-C-0076 F/G 20/4 NL

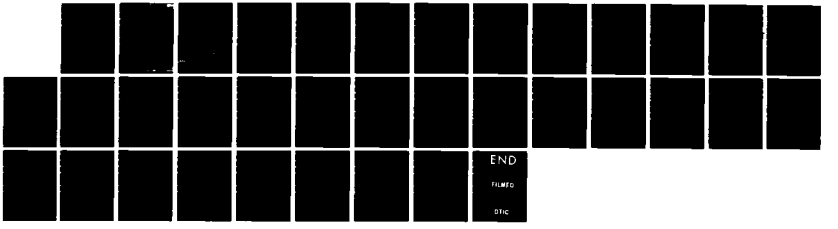

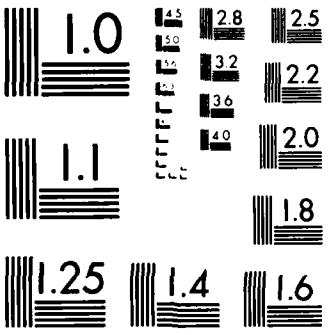

APPENDAGE EFFECTS ON PROPELLER INFLOW

SAIC-85/1008

SCIENCE APPLICATIONS, INC.

APPENDAGE EFFECTS ON PROPELLER INFLOW

SAIC-85/1008

SAIC

Science Applications International Corporation

34 Holiday Court, Suite 318, Annapolis, Maryland 21401, (301) 266-0991

APPENDAGE EFFECTS ON PROPELLER INFLOW

SAIC-85/1008

Contract #N00014-84-C-0076

15 January 1985

Submitted to

David W. Taylor Naval Ship
Research & Development Center
Code 1505
Bethesda, MD

Submitted by

G.H. Christoph
C.H. von Kerczek

APPROVED FOR PUBLIC RELEASE
DISTRIBUTION UNLIMITED

SCIENCE APPLICATIONS INTERNATIONAL CORPORATION

134 Holiday Court, Suite 318
Annapolis, Maryland 21401
(301) 266-0991; D.C. - 261-8026

SAIC
Science Applications
International Corporation

UNCLASSIFIED

SECURITY CLASSIFICATION OF THIS PAGE (When Data Entered)

REPORT DOCUMENTATION PAGE		READ INSTRUCTIONS BEFORE COMPLETING FORM
1. REPORT NUMBER	2. GOVT ACCESSION NO. AD-A152 396	3. RECIPIENT'S CATALOG NUMBER
4. TITLE (and Subtitle) Appendage Effects on Propeller Inflow		5. TYPE OF REPORT & PERIOD COVERED Final - 10/24/83 - 10/24/84
		6. PERFORMING ORG. REPORT NUMBER SAIC-85/1008
7. AUTHOR(s) G.H. Christoph C.H. von Kerczek		8. CONTRACT OR GRANT NUMBER(s) N00014-84-C-0076
9. PERFORMING ORGANIZATION NAME AND ADDRESS Science Applications International Corporation 134 Holiday Court, Suite 318 Annapolis, Maryland 21401		10. PROGRAM ELEMENT, PROJECT, TASK AREA & WORK UNIT NUMBERS
11. CONTROLLING OFFICE NAME AND ADDRESS David W. Taylor Naval Ship Research and Development Center, Code 1505 Bethesda, Maryland 20084		12. REPORT DATE 15 January 1985 13. NUMBER OF PAGES 31
14. MONITORING AGENCY NAME & ADDRESS(if different from Controlling Office) Office of Naval Research 800 N. Quincy Street Arlington, Virginia 22217		15. SECURITY CLASS. (of this report) UNCLASSIFIED 15a. DECLASSIFICATION/DOWNGRADING SCHEDULE N/A

16. DISTRIBUTION STATEMENT (of this Report)

Approved for Public Release: Distribution Unlimited

17. DISTRIBUTION STATEMENT (of the abstract entered in Block 20, if different from Report)

18. SUPPLEMENTARY NOTES

This research was sponsored by the Naval Sea Systems Command General Hydrodynamics Research Program, administered by the David W. Taylor Naval Ship Research and Development Center (Code 1505), Bethesda, MD 20084.

19. KEY WORDS (Continue on reverse side if necessary and identify by block number)

GHR Program, Boundary Layers, Ships, Appendage Drag, Propeller inflow, Wakes, Viscous Drag

20. ABSTRACT (Continue on reverse side if necessary and identify by block number)

A simplified method for computing the propeller inflow velocity on ships with propellers mounted on the side or underneath, such as destroyers, is developed. The method utilizes the superposition of quasi-two-dimensional wake calculations of struts and shafts and the accurate calculation of the nominal 3-D boundary layer and potential flow that occurs on the bare hull. It is possible to calculate the nominal flow for these cases because the propellers are mounted forward of the stern region. There the thin boundary layer calculation methods are valid.

DD FORM 1 JAN 73 1473 EDITION OF 1 NOV 65 IS OBSOLETE

S/N 0102-LF-014-6601

UNCLASSIFIED

SECURITY CLASSIFICATION OF THIS PAGE (When Data Entered)

ABSTRACT

A simplified method for computing the propeller inflow velocity on ships with propellers mounted on the side or underneath, such as destroyers, is developed. The method utilizes the superposition of quasi-two-dimensional wake calculations of struts and shafts and the accurate calculation of the nominal 3-D boundary layer and potential flow that occurs on the bare hull. It is possible to calculate the nominal flow for these cases because the propellers are mounted forward of the stern region. There the thin boundary layer calculation methods are valid.

TABLE OF CONTENTS

LIST OF FIGURES

LIST OF TABLES

LIST OF SYMBOLS

A	Frontal Area
b	Wake half width
c	Chord
C	Defined by eq. (11)
c_f	Skin-friction coefficient, = $2\tau_w/(\rho_e u_e^2)$
c_D	Drag coefficient, = $2D/(\rho u_e^2 A)$
d	Diameter
D	Drag
F(G)	Entrainment function, eq. (4)
g	Function defined by eq. (14)
H	Shape factor
K	Constant, = 0.41
q	Entrainment variable, eq. (2)
r/R	Percent of propeller radius
R_d	Reynolds number, = $u_e d/\nu$
Re_θ	Reynolds number, = $u_e \theta/\nu$
t	Thickness
u	Streamwise velocity
u*	Friction velocity, = $(\tau_w/\rho)^{1/2}$
W	Velocity defect, = $u_e - u$
W_o	Maximum velocity defect, = $u_e - u_{CL}$
x	Longitudinal coordinate
x*	Nondimensional coordinate, = $u^* x/\nu$

y	Normal coordinate
δ	Boundary-layer thickness
δ^*	Displacement thickness
η	Far-wake coordinate, = y/b
θ	Momentum thickness
ν	Kinematic viscosity
ρ	Density
τ_w	Wall shear stress

Subscripts

ave	Average
b.l.	Boundary layer
CL	Centerline
e	Boundary layer edge
t.e.	Trailing edge

Section 1
INTRODUCTION

An analytical method for predicting the flow around and in the wake of hull appendages is desirable due to the scaling difficulties inherent in appended model testing. The flow around the appendages is Reynolds number (R_n) dependent and is not correctly extrapolated to full-scale by Froude number (F_n). An analytical solution for the viscous flow around an appended hull is difficult due to flow separation around the appendages at R_n of interest ($10^4 \leq R_n \leq 10^9$) and the fact that parts of the appendages are embedded in the hull boundary layer. It is not yet feasible to solve the Navier-Stokes equations for flow around appendages on the hull so that approximate techniques should be developed. For certain hull appendage configurations, such as destroyer hull propeller shafts and shaft support struts, approximate calculation methods can be worked out. Such methods that can predict fairly accurate values of the propeller inflow would be extremely valuable for design purposes. The fact that on destroyer hulls the propellers are not completely immersed in the hull boundary layer and that hull-appendage interference effects are not in the way of the propeller are reasons why simple approximate models for the propeller inflow may be feasible. The main problem to solve in this case is obtaining an accurate description of the nominal flow over the hull (including wave effects) with the appendages removed. This nominal flow is needed to trace the path of the appendage wakes which are largely two-dimensional and can be fairly accurately calculated. For destroyer hull forms it is not necessary to deal with complicated stern shapes, such as cruiser sterns, because the propellers are well forward of the stern. It is only necessary to calculate the nominal flow over the hull forward of the stern precisely in the region where current 3-D boundary layer and potential flow methods work well.

For application to ships whose propellers are mounted along-side of the hull and ahead of the stern, this study develops a simplified method for computing the flow into a propeller. This flow is only partially disturbed by the hull boundary layer but can be substantially disturbed by the appendage wakes.

Section 2
TECHNICAL APPROACH

Recently SAIC has been engaged in making bare hull viscous flow calculations for the DDG 51 destroyer hull form (von Kerczek, et al., 1983, and Stern and von Kerczek, 1983). Figure 1 shows the DDG 51 stations in way of the propeller and the shaft support struts. Also shown is the propeller disc and the calculated nominal boundary thickness at the propeller station for both model and full-scale and for the 30-knot full-scale speed condition. It can be seen in Figure 1 that for model-scale most of the propeller disc is outside the bare hull boundary layer and that for full-scale all of the propeller disc is outside the bare hull boundary layer. It is also evident that the wake from the propeller shaft and shaft support struts flows directly into the propeller disc. The experimental nominal wake results for the DDG 51 (Dawson, 1982) confirm that most of the wake deficit is due to wake from the appendages. It is also indicated by Dawson that the wake velocities are about 10% higher than the model speed near the lower part of the propeller disc. This is probably due to free surface effects and implies the need for including such effects in the bare hull potential flow calculation. Also note that the strut/hull intersection is about one propeller radius above the propeller disc.

Based on the above observations the following model is proposed. It is assumed that the primary effects of the interaction between the bare hull and the appendage boundary layers is that the appendage boundary layer/wake development is driven not just by the external potential flow but by the local velocity. This local velocity may be the hull boundary layer for those parts of the appendage located close to the hull or the external potential flow for those parts of the appendage well outside the boundary layer. A further approximation is to superpose results from two-dimensional strut and shaft section wake calculations at different propeller radii. This is justified by the low value of local flow sweep angle on the struts indicated by the bare hull viscous flow solution. Unfortunately, funding constraints did not permit free surface effects to be included. However, future effort should be directed towards including free surface effects.

Table I

WAKE DEFECT PREDICTIONS DUE TO STRUTS

CONDITION	r/R	WAKE WIDTH AT PROPELLER PLANE	AXIAL VELOCITY RATIO AT WAKE CENTERLINE
Full Scale	0.633	12.3^{o}	0.82
Full Scale	0.781	10.0^{o}	0.82
Full Scale	0.963	8.1^{o}	0.82
Model Scale	0.633	14.3^{o}	0.73
Model Scale	0.781	11.6^{o}	0.73
Model Scale	0.963	9.4^{o}	0.73

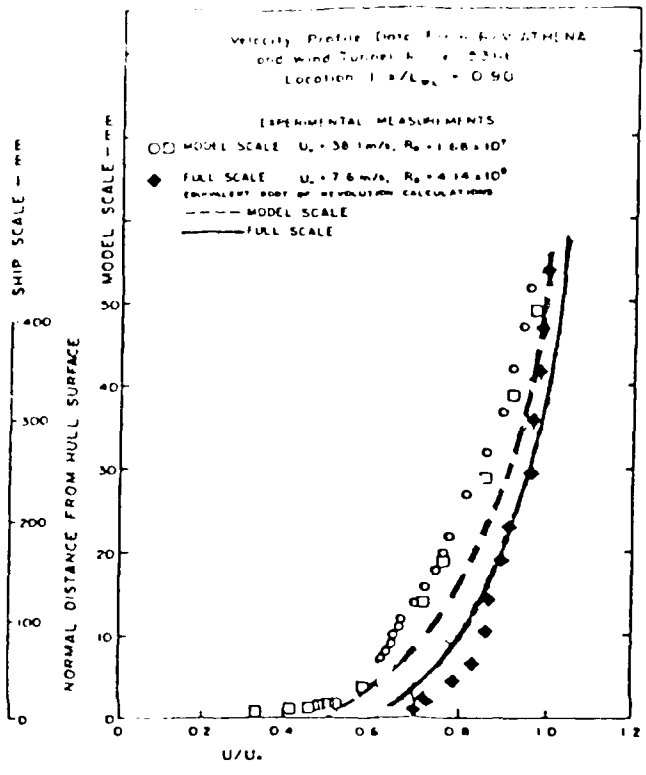

Figure 5: Measured and calculated boundary layer velocity profiles for ATHENA.

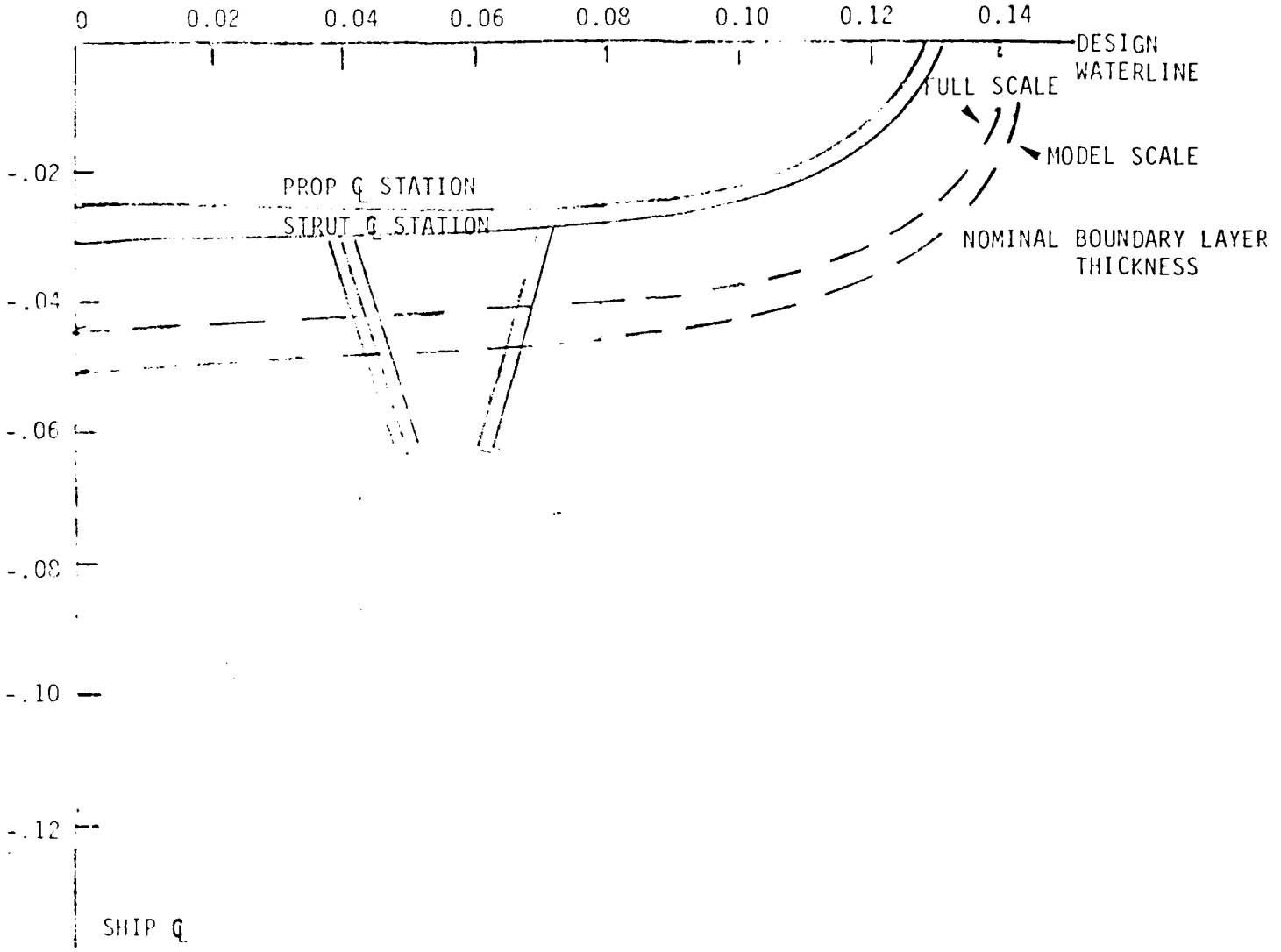

Figure 4: ATHENA stations in way of the propeller and the shaft support struts.

The strut and shaft wake analyses presented in this report were compared to the Reed and Day (1979) data for the longitudinal velocity in the propeller plane. Comparisons are presented at propeller radii of r/R = 0.633, 0.781, 0.963. No attempt was made to compare at the innermost radius, r/R = 0.456, because of the complicated flow pattern and large scatter in the data. In order to apply the wake analyses, the bare hull potential-flow and boundary-layer solutions are required. The SAIC potential-flow and boundary-layer codes (von Kerczek, 1982) were run at model and full-scale conditions. The small-crossflow option was used for the boundary-layer solution. Calculated nominal boundary-layer thicknesses at the propeller station are plotted in Figure 4. As can be seen, most of the propeller disk lies outside of the boundary layer. In Figure 5, comparisons are shown for the computed and measured velocity profiles at x/L = 0.9. The present velocity profile predictions are similar to those given in Reed and Day (1979). That is, the full-scale profile is in good agreement but the predicted model profile is too full.

The struts on the Athena were Navy EPH sections with a chord to thickness ratio of six. For the results of this report, the struts were modeled by an NACA 0021 airfoil section. This was for convenience because the geometry and potential flow were available. Since both sections are similar in shape, it is felt that this approximation will have a negligible effect on the predicted wake defects. For initialization of the wake calculations, Head's boundary-layer equations were integrated over the NACA 0021 airfoil section for model and full-scale conditions. In both cases, the airfoil sections were assumed fully turbulent. In reality, there was probably considerable laminar flow (perhaps one-half the airfoil) on the model section. For full-scale and model-scale conditions, the velocity defect due to the strut was overpredicted, as shown in Table I. Due to the scaling, wake defects appear as spikes when plotted as in Figure 6. Similar results were obtained by Reed and Day (1979). A predicted wake profile at the propeller plane is shown in Figure 7. Most of the velocity defect in the propeller plane is due to the shaft. For the shaft inclined at 10^{o} to the flow, the stream sees elliptical sections of $c/t \approx 6$. Reynolds numbers based on shaft diameter are

Section 4
SAMPLE CALCULATION

Comparisons were made to the data and computations of Reed and Day (1979). In their experiment, they measured the wake and boundary layer on a full-scale twin-screw displacement ship - The Athena. The full-scale wake measurements were taken at four radii in the propeller plane and the full-scale boundary-layer profiles were obtained at three longitudinal locations with and without the propeller operating. The model-scale nominal wake was determined in a towing tank using pitot tubes while the model-scale boundary-layer measurements were made in a wind tunnel using hot wire anemometers.

For their calculations, Reed and Day (1979) decomposed the velocity in the propeller disk as follows:

Velocity = uniform stream
+ perturbation due to hull shape
+ perturbation due to boundary-layer displacement effect
+ viscous wake of struts
+ viscous wake of shafting.

They found a negligible effect of the hull potential flow on the propeller plane velocities. Since the boundary-layer displacement thickness increased the hull thickness by less than one percent of beam, the boundary-layer displacement effect was neglected. The velocity defect caused by the struts was predicted using an empirical far-wake formulation. Their calculated velocity defects due to struts significantly overpredicted the velocity defects that were observed on either model or full scale. Reed and Day (1979) estimated the wake behind the shaft by a relationship between the base pressure of an inclined circular cylinder to the velocity defect in the wake. They predicted the shaft wake to be less than two percent of model speed and one percent of ship speed. These were significantly less than measured values.

Section 3
PROCEDURE FOR OBTAINING PROPELLER PLANE VELOCITIES

The following procedure is recommended for calculating velocities in the propeller plane, including appendage effects.

1. Calculate the potential flow around the ship without appendages.

2. Calculate the 3-D boundary layer over the ship without appendages.

3. From a particular location on the appendage, trace the streamline to the propeller plane.

4. For a particular location on the appendage, find u/u_e from the ship boundary layer solution.

5. Use this value of u/u_e to drive the appendage wake calculations.

6. At the propeller plane

$$u = u_e \left(\frac{u}{u_e}\right)_{b.l.} \left(\frac{u}{u_{scale}}\right)_{wake}$$

where the potential flow velocity u_e is taken at the propeller.

that on most ships, except near the propeller hub, the propeller plane can be considered to be in the far wake of the shaft. It is known that in the 2-D turbulent far wake of cylinders, the wake width $b \propto x^{1/2}$ and the wake centerline velocity $u_{CL} \propto x^{-1/2}$. Similarity solutions can be obtained, e.g., Schlichting (1968). Constants based on Schlichting's (1968) measurements for wakes behind circular cylinders of diameter d, give

$$b = 0.569\ (xC_D d)^{1/2}\ ,$$

$$\frac{W}{u_e} = 0.976\ \left(\frac{x}{C_D d}\right)^{-1/2} \left[1 - (y/b)^{3/2}\right]^2 \qquad (22)$$

where

$$W = u_e - u,$$

$$C_D = \frac{2D}{\rho u_e^2 A}\ ,\ A = \text{frontal area}\ .$$

From Schlichting's measurements these formulas are accurate for

$$\frac{x}{C_D d} > 50$$

Since the shaft is inclined at some angle to the flow (typically about 10^o), the drag coefficient C_D should be for elliptical sections. Hoerner (1969) presents equations for drag coefficients of elliptical sections. They are

$$C_D = 0.015\ (1+c/t) + 1.1\ (t/c) \qquad \text{for } uc_e/\nu < 1\text{x}10^5$$

$$C_D = 0.005\ (4+2(c/t) + 120\ (t/c)^2) \qquad \text{for } uc_e/\nu > 1\text{x}10^5 \qquad (23)$$

where c/t is the chord to thickness ratio. For wake calculations presented in this report, the virtual origin was taken at the shaft centerline.

$$c_{f_{ave}} = \frac{1}{L}\int_0^L c_f \, dx \tag{17}$$

For a flat plate, the Blasius turbulent skin-friction formula yields

$$c_{f_{ave}} = 1.25\ c_f(L) \tag{18}$$

where the local value of c_f has been evaluated at the plat length L. If

$$\frac{u_e}{u^*_{ave}} = \left(\frac{2}{c_{f_{ave}}}\right)^{1/2}, \tag{19}$$

one obtains

$$u^* = u^*_{ave}/(1.25)^{1/2} \tag{20}$$

for a flat plate. This relationship for u*, equation (20), is substituted into Alber's equations (13) and (15). It is assumed that the use of u^*_{ave} in Alber's (1980) equations is a good representation for u_{CL} for airfoil wakes, although the authors were unable to obtain data for comparisons.

Once the wake centerline velocity and wake width have been calculated, a wake velocity profile can be obtained. Ramaprian et al. (1982) found that the velocity defect profile in far-wake coordinates

$$\frac{W}{W_o} = \text{EXP}\left[-4\eta^2 \ln 2\right], \ \eta = y/b \tag{21}$$

accurately represents wake data, even for $x/\theta = 25$. This formulation was considered sufficient for the present applications. In equation (21), $W = u_e - u$ is the velocity defect, $W_o = u_e - u_{CL}$ is the maximum velocity defect, and b is the wake half width.

The flow over an inclined shaft is fully separated and thus is computationally difficult. Such a calculation was beyond the scope of this task. Instead the following approximate procedure was employed. First, it is noted

where u_{CL} is the wake centerline velocity and u* is the friction velocity at the plate trailing edge. Ramaprian et al. (1982) show that the equation suggested by Alber (1980) is more accurate when compared to the data sets of Ramaprian et al. (1982), Pot (1979), Andreopoulos (1980) and Chevrey and Kovasznay (1969). Alber (1980) obtained an analytical solution using an inner and outer layer coordinate expansion technique. It appears accurate to x* greater than $2x10^5$. Alber's (1980) equation is

$$\frac{u_{CL}}{u^*} = \frac{1}{K}\left[\ln g(x^*) - \gamma\right] + B \qquad (13)$$

where K = 0.41, γ = 0.5772157 (Euler constant), B = 5.0. The function g is defined by

$$g(x^*)\left[\ln g(x^*) - 1\right] = K^2 x^* \ . \qquad (14)$$

In the central portion of the wake immediately downstream of the trailing edge, Alber assumed the flow to be laminar and recovered the Goldstein solution

$$\frac{u_{CL}}{u^*} = 1.61\ x^{*1/3} \ . \qquad (15)$$

This solution is valid until the inner wake grows to equal the upstream sublayer thickness. The streamwise extent of this region is on the order of ten sublayer thicknesses. Equations (13) and (15) match at approximately x* = 300, so this will be the crossover criterion used. In its present form, the u_{CL} calculation is based on u* determined from the local c_f evaluated at the plate trailing edge from

$$\frac{u_e}{u^*} = (2/c_f)^{1/2} \ . \qquad (16)$$

For an airfoil this is a problem since c_f, and hence u*, tends to zero very rapidly near the trailing edge. To avoid this problem, Alber's (1980) correlation is evaluated with u* based on $c_{f_{ave}}$ where

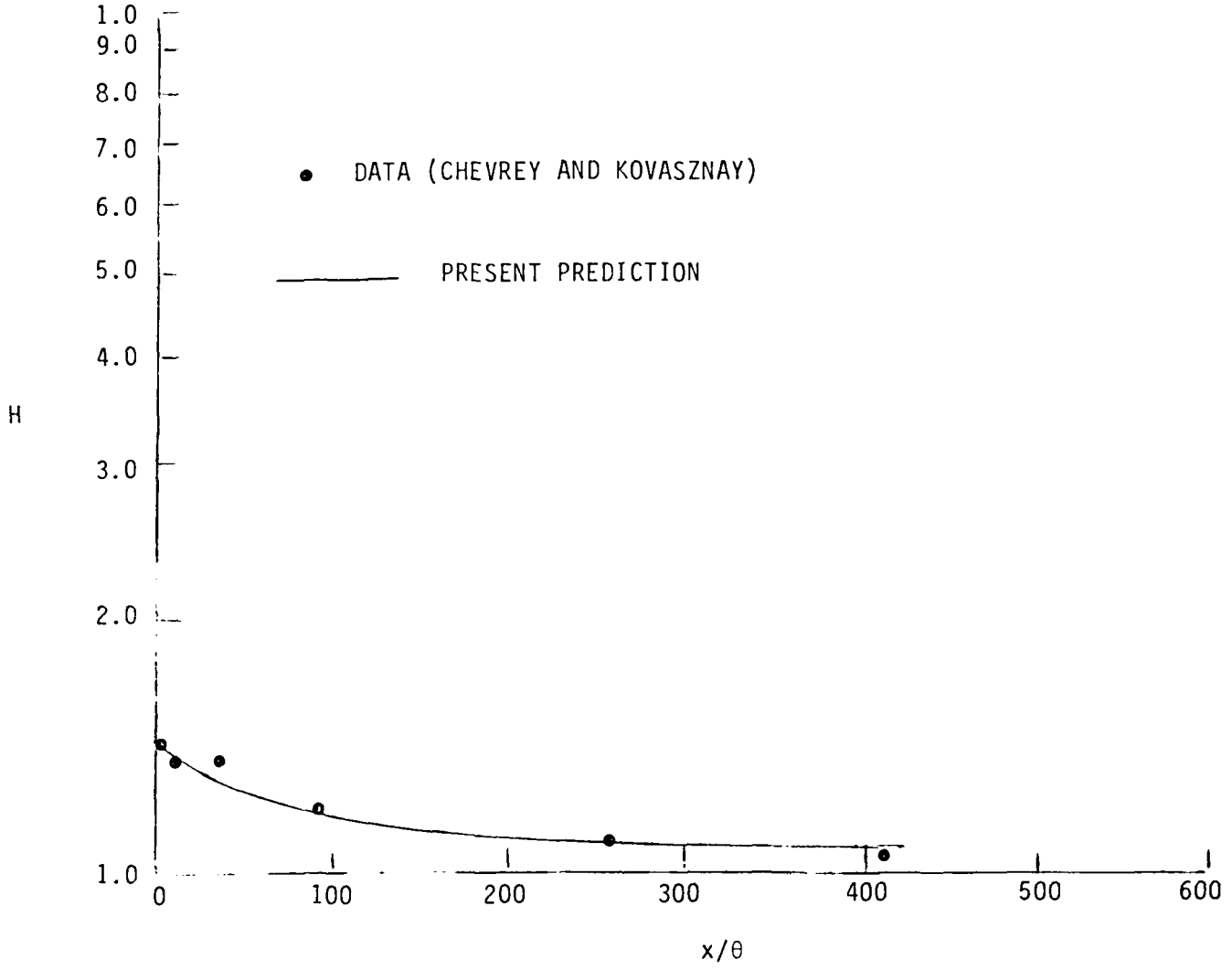

Figure 3: Wake shape factor comparison.

known from measurements. Adjustment of the wake entrainment rate follows the work of Green (et al., 1973). From Green's analysis, just downstream of the trailing edge

$$\theta \frac{dH}{dx} = -0.06\ (H-1)^3\ , \tag{8}$$

while in the far wake

$$\theta \frac{dH}{dx} = -0.242\ (H-1)^3\ . \tag{9}$$

Here θ is the half-wake momentum thickness. Based on the findings of Ramaprian et al. (1982), flat plate far wake conditions are obtained when x/θ is greater than 350. It was decided to adjust the wake entrainment by calculating it from an equation of the form

$$\theta \frac{dH}{dx} = C\ (H-1)^3 \tag{10}$$

The constant C is linearly interpolated from its trailing edge (t.e.) value (-0.06) to its far wake value (-0.242), by

$$C = \frac{-0.06\ (350 - x_o/\theta) - 0.242\ (x_o/\theta)}{350} \tag{11}$$

where $x_o = x - x_{t.e.}$. Comparison of the calculated H to the flat plate wake data of Chevrey and Kovasznay (1969) is shown in Figure 3. Agreement is seen to be excellent. Integration of equations (1), (2) and (10) (with c_f=0) along with equation (7) provides the wake width. Additional calculations are needed to obtain the wake velocity profile and centerline velocity.

Both Andreopoulos and Bradshaw (1980) and Alber (1980) have suggested wake centerline velocity correlations of the form

$$u_{CL}/u^* = u_{CL}/u^*\ (x^* = u^*x/\nu) \tag{12}$$

$$\frac{d\theta}{dx} = c_f/2 - (H+2)\frac{\theta}{u}\frac{du}{dx} \quad . \tag{1}$$

The boundary-layer entrainment equation is

$$\frac{dq}{dx} = F(G) - \frac{q}{u}\frac{du}{dx} \tag{2}$$

where

$$G = 1.535\ (H-0.7)^{-2.715} + 3.3 \tag{3}$$

and

$$F(G) = 0.0306\ (G-3.0)^{-0.653} \quad . \tag{4}$$

The skin-friction coefficient was modeled by the Ludwieg-Tillmann formula

$$c_f = 0.246 \times 10^{-0.678H}\ Re_\theta^{-0.268} \tag{5}$$

but any other $c_f = c_f(Re_\theta, H)$ could have been used. Since

$$G = (\delta-\delta^*)/\theta,\ q = G\theta \tag{6}$$

one obtains

$$\delta = q + \theta H \quad . \tag{7}$$

On many airfoils the flow separates near the trailing edge. Rather than attempt to calculate through separation, the wake calculations are started at the location of separation. The turbulent wake from the airfoil trailing edge to the propeller plane is calculated using basically the same method as for the turbulent boundary layer with the following additions. The wake centerline is assumed to follow the bare hull potential flow streamline from the airfoil trailing edge to the propeller plane. In the wake the skin-friction is zero and the wake entrainment rate is adjusted to approach its far wake value

The calculation of the boundary layer/wake of a strut (or shaft) section is a four-step procedure (see Figure 2).

(1) Calculate laminar boundary layer from the strut leading edge stagnation point to the point of transition to turbulent flow, x_{tr}.

(2) Determine x_{tr}.

(3) Calculate turbulent boundary layer from x_{tr} to the strut trailing edge, x_{te}.

(4) Calculate turbulent wake from x_{te} to propeller plane.

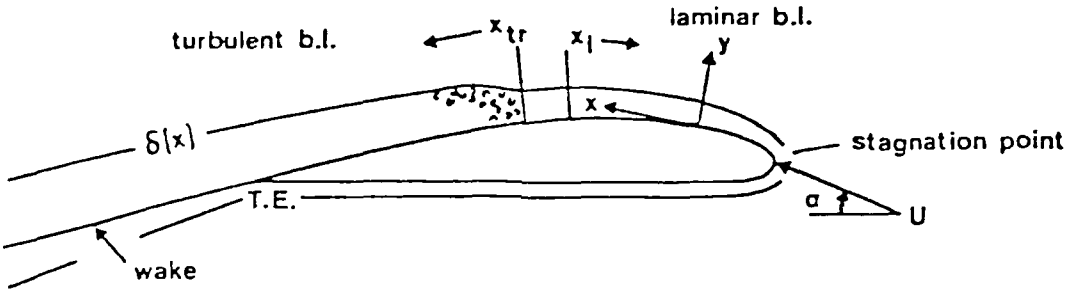

Figure 2: Sketch of strut-section boundary layer/wake.

For the present calculations the flow over the appendages has been assumed all turbulent. Two types of appendages are considered: struts and shafts.

The turbulent boundary layer over the struts is calculated using Head's (1958) momentum integral entrainment method. For a 2-D flow, the momentum integral equation is

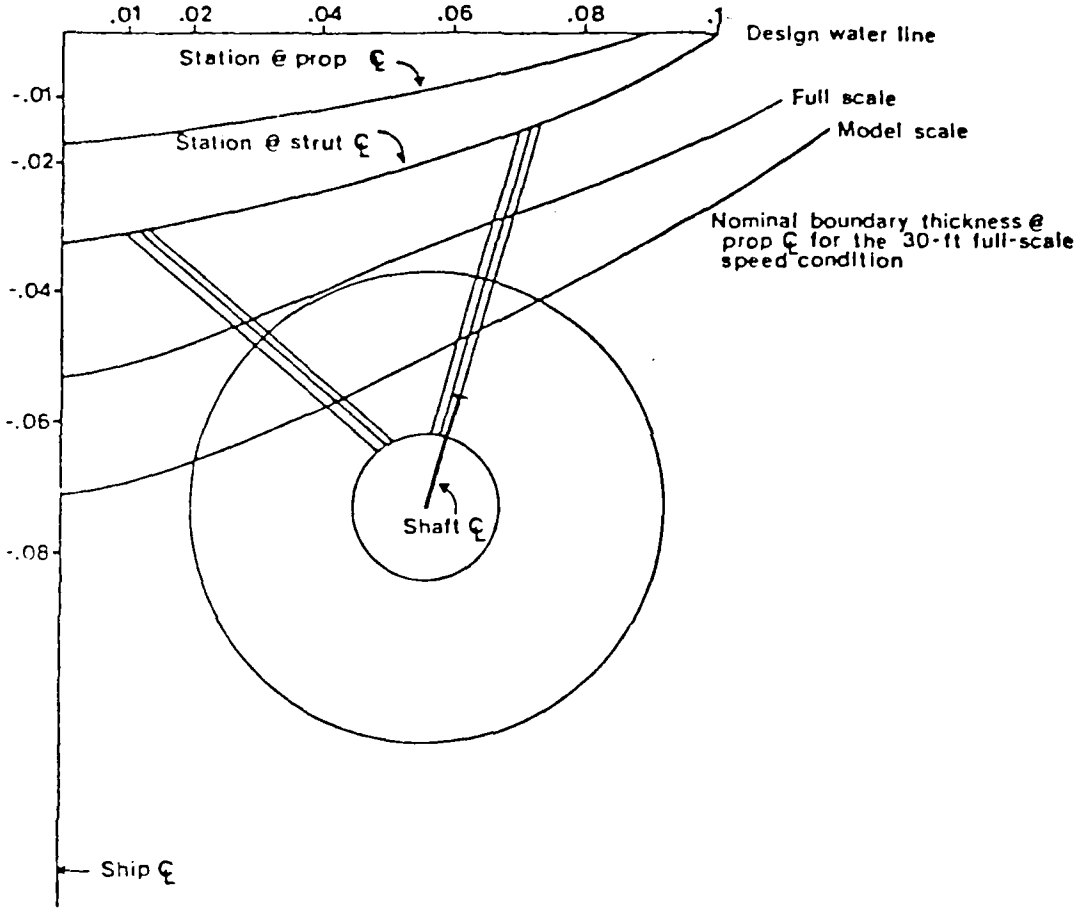

Figure 1: DDG 51 stations in way of the propeller and the shaft support struts.

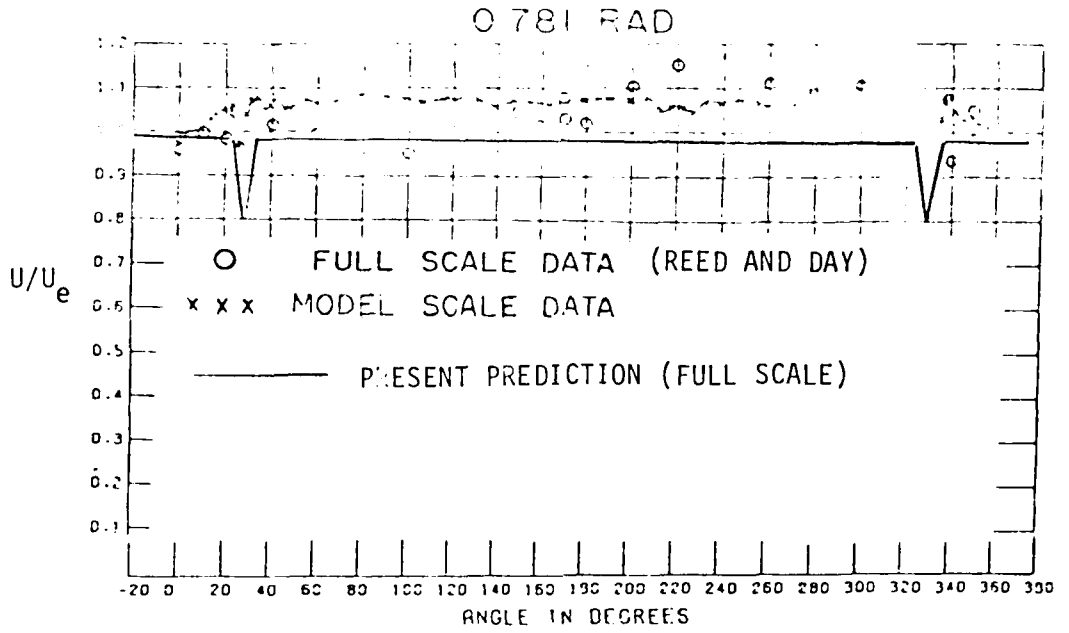

Figure 6: Wake streamwise velocity ratio for ATHENA - full scale strut effect.

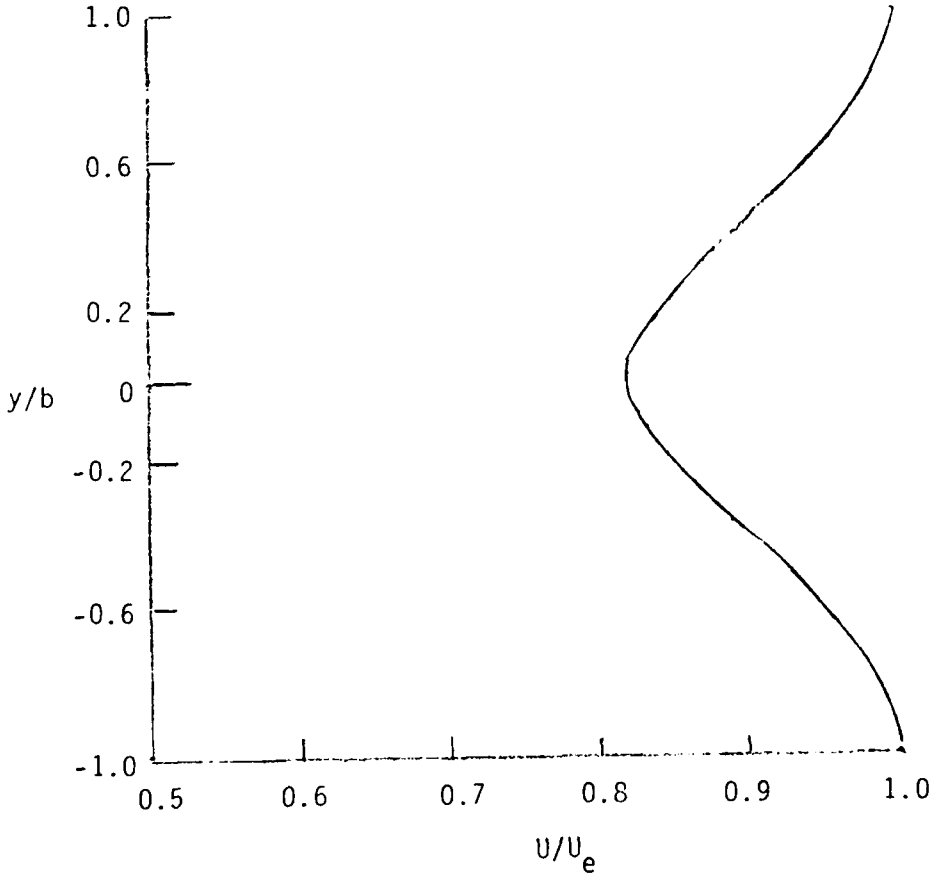

Figure 7: Typical wake profile prediction.

$$R_d = ud/\nu = 1.6 \times 10^6 \quad \text{full scale}$$
$$= 6.7 \times 10^4 \quad \text{model scale.}$$

Then, formulas (23) give

$$C_D = 0.1 \quad \text{full scale}$$
$$C_D = 0.3 \quad \text{model scale.}$$

The wake half width and velocity defect were calculated from equation (22). These results are plotted in Figures 8-10 for full scale and Figures 11-13 for model scale. The wake widths seem correct for both model and full scale, but the wake defect for the model scale is too large. Of course, all the data lie above the predictions because of free surface effects.

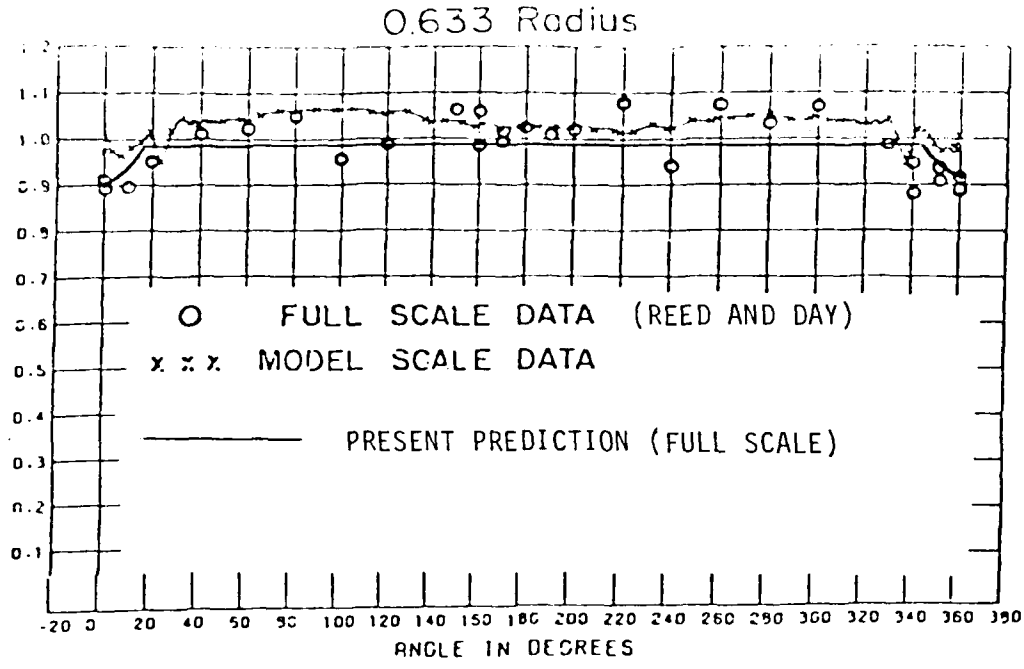

Figure 8: Wake streamwise velocity ratio for ATHENA - full scale shaft effect at 0.633 radius.

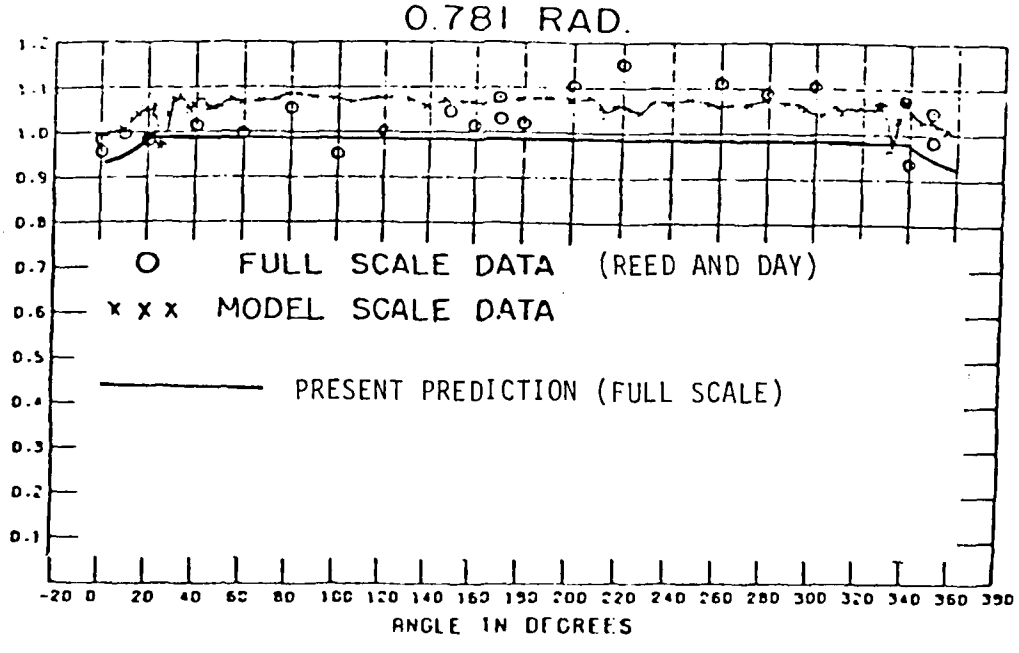

Figure 9: Wake streamwise velocity ratio for ATHENA - full scale shaft effect at 0.781 radius.

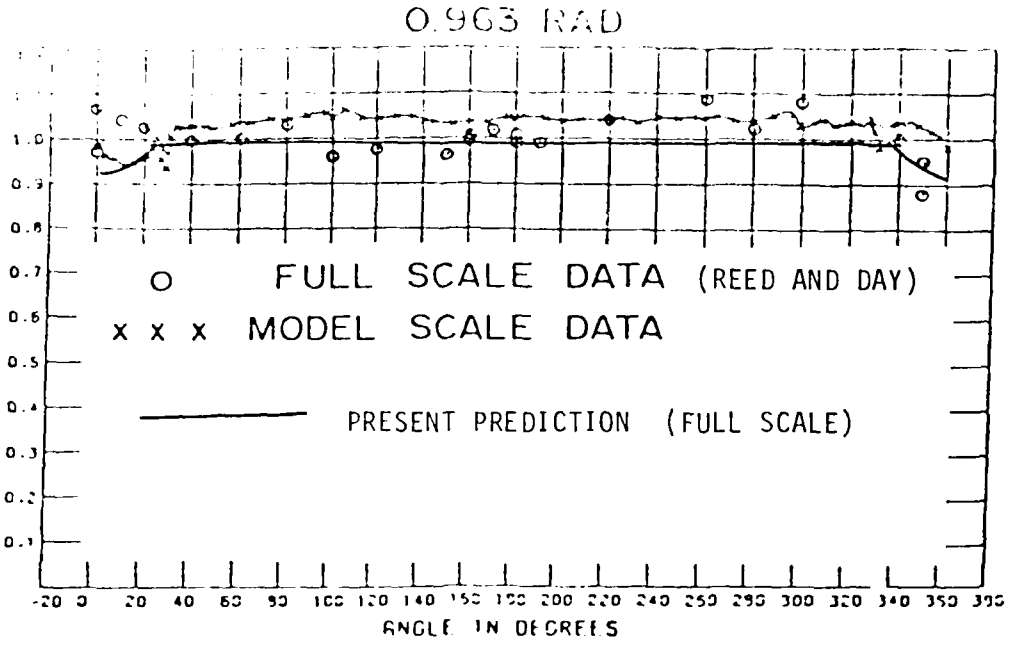

Figure 10: Wake streamwise velocity ratio for ATHENA - full scale shaft effect at 0.963 radius.

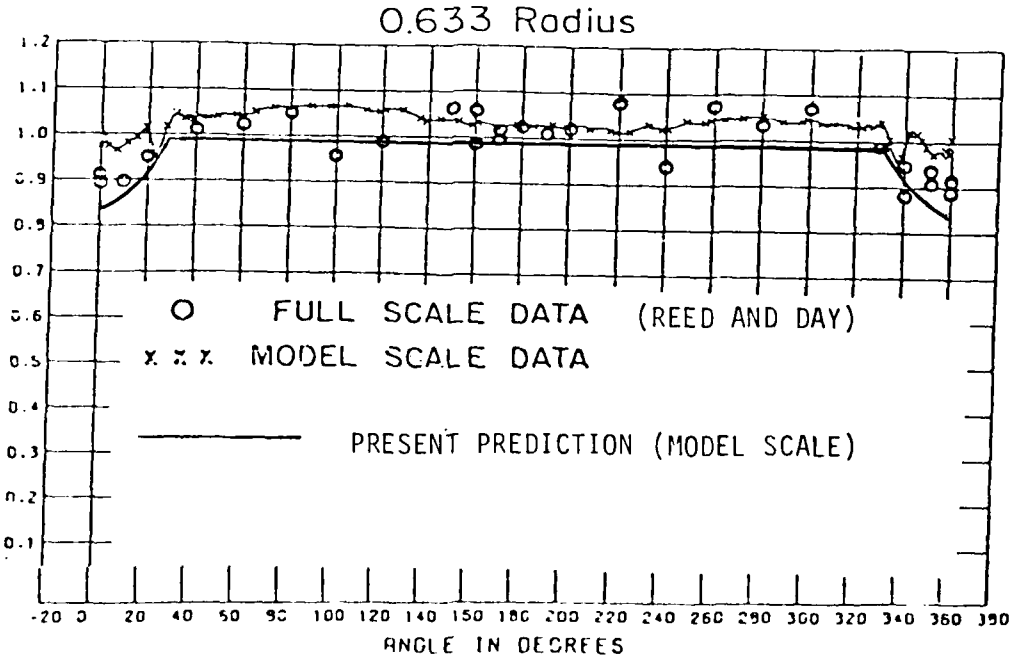

Figure 11: Wake streamwise velocity ratio for ATHENA - model scale shaft effect at 0.633 radius.

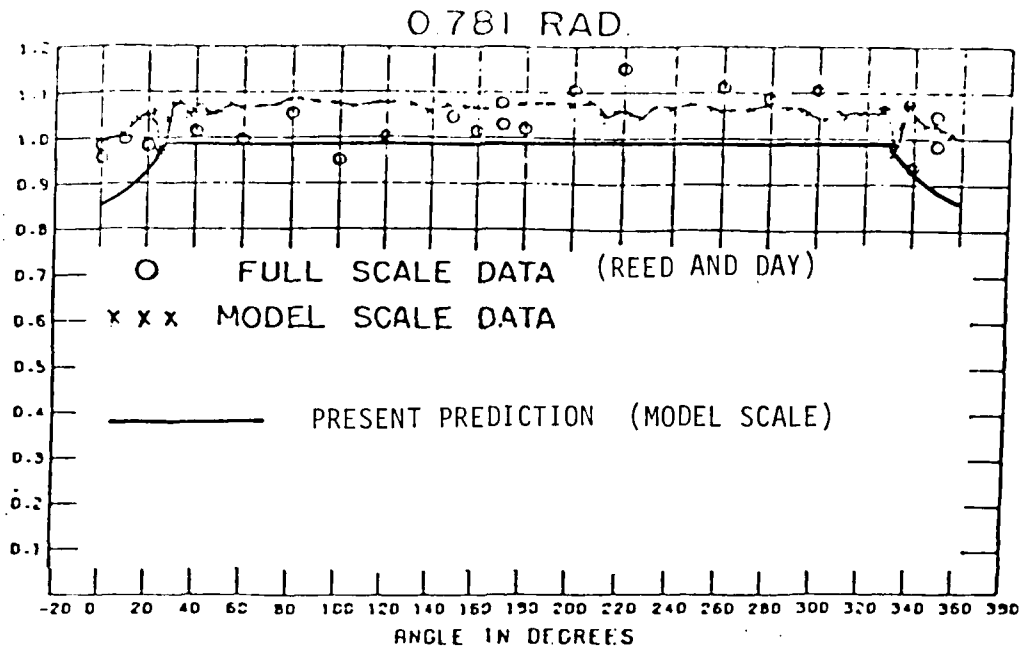

Figure 12: Wake streamwise velocity raito for ATHENA - model scale shaft effect at 0.781 radius.

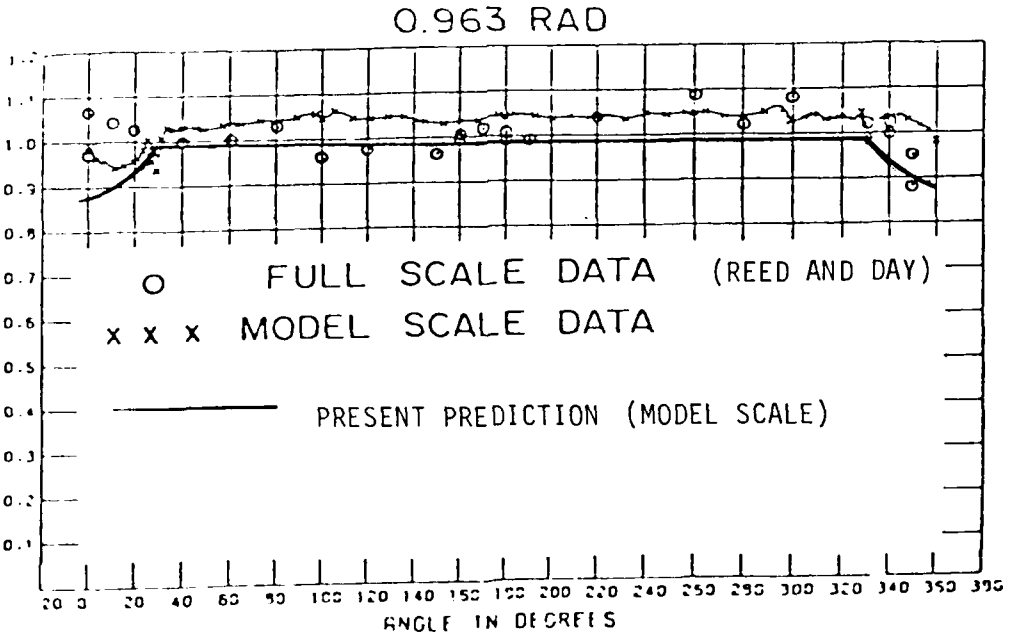

Figure 13: Wake streamwise velocity ratio for ATHENA - model scale shaft effect at 0.963 radius.

Section 5
CONCLUSIONS

Based on the available data it is not possible to assess fully the effectiveness of the appendage wake calculation method presented here. The comparisons between the calculated and measured wakes do show fair agreement. However, the measurements do seem sufficiently erratic, especially the full scale ones, that better agreement can hardly be expected. Since the appendage affect on propeller inflow is not large, the fair agreement obtained by the calculation method may be adequate, at least for the purpose of powering predictions. However, for the purpose of predicting vibration and noise characteristics of the propeller, where the harmonic distribution of wake defect is important, more accurate procedures may be desirable.

What does seem clear in the experiments is that the propeller inflow is mainly affected by the potential flow and geometry of the hull in the vicinity of the propeller disks. It seems important to include wave effects since the local velocity is substantially affected by waves. Unfortunately funding for this project did not include means to calculate the full free surface wave effects on propeller inflow.

It seems worthwhile to obtain more experimental data on appendage wake effects to further validate and improve the tool developed in this effort. Once the present tool is proved to be uniformly reliable to at least the accuracy indicated here then it should prove useful to designers for evaluation purposes.

Section 6

REFERENCES

Alber, I.E. (1980): AIAA Journal, Vol. 18, pp. 1044-1051.

Andreopoulos, J. (1978): Ph.D. Thesis, Dept. of Aeronautics, Imperial College, London.

Andreopoulos, J. and Bradshaw, P. (1980): J. Fluid Mech., Vol. 100, pp. 639-668.

Chevrey, R. and Kovasznay, L.S.G. (1969): AIAA Journal, Vol. 7, pp. 1641-1643.

Dawson, D.M. (1982): DTNSRDC Report SPD-0200-04.

Green, J.E., Weeks, D.J. and Brooman, J.W.F. (1973): Reports and Memoranda No. 3791, Aerodynamics Dept., R.A.E., Farnborough.

Head, M.R. (1958): Aeronautical Research Council, London RM-3152.

Hoerner, S.F. (1965): "Fluid-Dynamic Drag," published by the author.

Pot, P.J. (1979): Data Report, NLR TR-79063 U, The Netherlands.

Ramaprian, B.R., Patel, V.C. and Sastry, M.S. (1982): AIAA Journal, Vol. 20, pp. 1228-1235.

Reed, A.M. and Day, W.G. (1979): Twelfth Symposium, Naval Hydrodynamics, pp. 225-247.

Schlichting, H. (1968): "Boundary Layer Theory," McGraw-Hill, New York.

Stern, F. and von Kerczek, C. (1983): SAIC Report 463-83-408-LJ.

von Kerczek, C. (1982): SAIC Report 463-82-085-LJ.

von Kerczek, C., Scragg, C. and Stern, F. (1983): SAIC Report 463-83-398-LJ.

NAVAL SEA SYSTEMS COMMAND
GENERAL HYDROMECHANICS RESEARCH (GHR) PROGRAM
DISTRIBUTION LIST FOR TECHNICAL REPORTS

Addressee	Number of Copies
Commander David W. Taylor Naval Ship Research and Development Center Attn: Code 1505, Bldg. 14, Rm. 2 Bethesda, MD 20084-5000	20
Commander Naval Sea Systems Command Washington, D.C. 20360	
Attn: Mr. J. Sejd (SEA 05R24)	1
Mr. E. Comstock (SEA 55W3)	1
Mr. W. Sandberg (SEA 55W33)	1
Dr. C. Kennell (SEA 50151)	1
Mr. A. Chase (SEA 56X13)	1
Dr. T. Peirce (SEA 63R31)	1
Mr. A. Paladino (SEA 55N2)	1
Library (SEA 99612)	1
Dr. C.M. Lee, Code 432F Office of Naval Research 800 N. Quincy Street Arlington, VA 22217	1
Dr. George Lea, Room 1108 National Science Foundation 1800 G Street, N.W. Washington, D.C. 20550	1
Defense Technical Information Center Bldg. 5, Cameron Station Alexandria, VA 22314	12

END

FILMED

5-85

DTIC